Rate Constants of the Thermal Cis-Trans Isomerization of Azobenzene Dyes in Solvents, Acetone/Water Mixtures, and in Microheterogeneous Surfactant Solutions

KATHRIN GILLE, HELMUT KNOLL, KONRAD QUITZSCH

Wilhelm-Ostwald-Institut für Physikalische und Theoretische Chemie der Universität Leipzig, Linnéstr. 2, 04103 Leipzig, Germany

Received 22 October 1997; accepted 7 December 1998

Dedicated to Prof. Dr. Klaus Scherzer on occasion of his 65th birthday

ABSTRACT: Rate constants k_{iso} of the thermal cis-trans isomerization of four 4,4′-nitro-aminoazobenzenes with different amino groups have been determined in homogeneous aprotic solvents and polyglykol oligomers, primarily by means of conventional flash photolysis. The rate constants have been correlated with polarity (according to λ_{max} from UV/Vis absorption spectra of the trans isomers) and bulk viscosity of the solvents. Qualitative conclusions about the influence of varying concentrations of water with respect to polarity and hydrogen bonding on k_{iso}- and λ_{max}-values in acetone/water mixtures were derived. Based on these results the data from microheterogeneous solutions have been interpreted.

In microheterogeneous water/surfactant solutions k_{iso}-values of selected azo dyes were strongly dependent on the concentrations of SDS, Triton® X-100, $C_{12}EO_8$ in water, and varied with the composition of bicontinuous microemulsions of Igepal® CA-520/ heptane/water. The large spread of isomerization rate constants is in part due to varying microviscosity.

Replacement of H_2O by D_2O in aqueous surfactant solutions produced surprisingly large kinetic solvent isotope effects. © 1999 John Wiley & Sons, Inc. Int J Chem Kinet 31: 337–350, 1999

Correspondence to: H. Knoll

CCC 0538-8066/99/050337-14

INTRODUCTION

Microheterogeneous fluid reaction media (micellar and vesicular solutions, microemulsions) have been considered as simple models for biological reaction media [1] and are of practical importance in technical processes [2]. Their influence on the overall reaction rate of complex reactions compared with simple homogeneous solvents is due to concentration, separation, and diffusion effects within and between the microcompartments and across their extended interfaces. At the molecular level, the interface between the headgroups of surfactant or lipid molecules and water is of special interest. Reactivity at this interface, which is in fact an interfacial layer, is determined by the solvent structure around the probe molecule (in particular hydrogen bonding), polarity and viscosity.

There is a large number of spectroscopic studies in which probe molecules are added to characterize particular interfacial properties, for example, hydrogen bonding and polarity [3,4] and viscosity [5–7]. Reactivity parameters for the characterization of the local environment in microheterogeneous reaction media, however, have been studied less extensively [8–12].

Interpretation of rate constants of elementary reaction steps in microheterogeneous media, based on properties of the microenvironment determined by probe molecules, may be difficult if probe and reactant molecules are different, and may have a different microenviroment. Therefore, reactivity parameters of elementary reactions of molecules, which also exhibit spectroscopic probe properties with respect to the microenvironment in water-surfactant interface layers, are of interest.

The thermally stable trans isomers of donor-acceptor substituted azobenzene dyes show remarkable solvatochromy, and they can be easily transformed into the thermally unstable cis form by light. AM1 calculations show that the dipole moments of their cis isomers are about 6 D, similar to 8 D of the trans isomers [13]. Therefore, we assume that cis azobenzene dye molecules formed by the flash will remain essentially at the same sites as their trans form precursors. From UV/Vis spectroscopy it follows that this is the water-surfactant interface layer in most cases. So differences of the average microenvironment can be monitored by means of the UV/Vis absorption of the stable trans isomers. Moreover, the rate of the thermal cis-trans back isomerization is highly dependent on solvent properties in simple homogeneous solvents, and therefore, an appropriate model reaction for probing the water-surfactant interface layers by means of the reactivity parameter k_{iso} according to the following scheme:

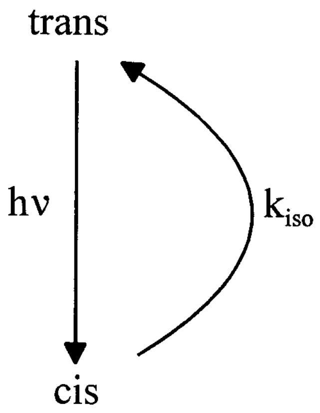

Scheme I

Schanze, Whitten et al. [14–18] studied the rates of thermal cis-trans isomerization of different 4,4’-nitro-aminoazobenzenes in simple solvents and different solutions of surfactants and lipids, in particular in reversed micelles of AOT, and mainly with 4,4’-nitro-diethylaminoazobenzene. These authors obtained a good correlation of $\Delta G^{\#}$-values of the cis-trans isomerization with the solvent polarity, and observed a rate increasing effect of hydrogen bond donating solvents. Steiner et al. [19] studied the thermal cis-trans isomerization of solvatochromic merocyanines and reported similar linear correlations between solvent polarity and isomerization rate constants.

In this study we repeated some experiments with 4,4’-nitro-diethylaminoazobenzene to show that our measurements are reliable, and we focused on the following new aspects:

1. We have chosen three azo dyes which differ at the amino group, to vary its electron donor capability, hydrogen bond formation ability, and rotor volume (Scheme II). By comparing the isomerization rate constants of different azo dyes in one solvent and of one azo dye in different solvents, conclusions can be drawn about the sensitivity of the isomerization rate constant on different properties of the medium.
2. Based on these results, the data from microheterogeneous solutions of mainly nonionic surfactants were evaluated with respect to the microenvironment of the probe molecules.
3. From the comparison of the rate constants of the thermal isomerization in H_2O/- and D_2O/surfactant solutions, respectively, conclusions are drawn on the accessibility of water to the react-

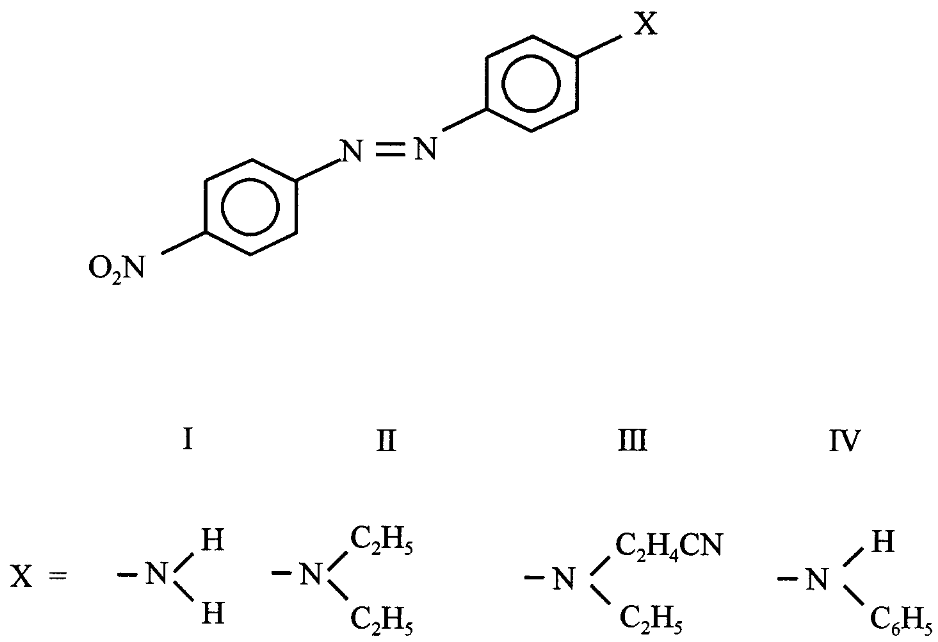

Scheme II

ing probe molecules and the importance of hydrogen bonding.

EXPERIMENTAL

Materials

4,4’-Nitro-aminoazobenzene (**I**, Aldrich), 4,4’-nitro-(ethyl-2-cyanoethyl)aminoazobenzene (**III**, Aldrich), have been used as received. 4,4’-Nitro-diethylamino-azobenzene (**II**) has been prepared according to [20]. 4,4’-Nitro-anilinoazobenzene (**IV**, Sigma) was dissolved in acetone and the solution decanted from the salt residue.

The following solvents were used as received: acetone (Merck, p.a. 0.01% water), acetonitrile, n-heptane (heptane), N,N-dimethylformamide (DMF, all Merck UVASOL), propionitrile and butyronitrile (Aldrich 99%), cyclohexane (Fluka 99.5%), Poly(-ethylenglycol) (PEO 600, Aldrich, average molecular weight 600), Poly(propylenglyol) (PPO 425, PPO 2000, Aldrich, average molecular weights 425 and 2000, respectively).

The following surfactants were used as received: sodiumdodecyl sulfate (SDS, Serva, p.a. recrystal. twice), t-octylphenyl-nona/decaethyleneglycolether/Triton® X-100 (triton X-100, Merck), p-iso-octylphenyl-pentaethylenglycolether/Igepal® CA-520 (igepal CA-520, Aldrich 98%), dodecyl-octaethylen-glycolether ($C_{12}EO_8$, Nikko). Water from a Milli-Q Plus apparatus (Millipore) and D_2O (Laborchemie Berlin, 99.7%) freshly distilled over $KMnO_4$ were used.

Apparatus

UV/Vis spectra and time-dependent measurements in the minutes range were carried out with a Lambda 2-spectrometer (Perkin-Elmer, $\Delta\lambda_{max}$ was estimated to ± 2 nm), irradiation for cis-trans isomerization with reaction times of minutes was performed by means of an argon ion laser Innova 305 (Coherent). For reaction times of microseconds to seconds a home-made microsecond flash-photolysis apparatus (FWHM 25 μs, up to 180 J/flash) equipped with a digital storage oscilloscope PM3533 (Fluke), and 5 or 10 cm cuvettes (water jacket, bath thermostat) was used. Bulk viscosities were taken from the literature [21] or measured for the polyglycol oligomers with a LS100 rheometer (Paar-Physica).

Procedures

From stock solutions of the azo dyes (10^{-3} mol dm^{-3}) in acetone, the desired aliquots were given to 10 ml volumetric flasks and the solvent evaporated. The samples were prepared from solvents or stock solutions of the surfactants, bicontinuous microemulsions, and water, respectively. The volumetric flasks were agitated in an ultrasonic bath and were allowed to let stand overnight. The concentrations of the azo dyes were between 2 and 5×10^{-6} mol dm^{-3} for the kinetic measurements, respectively.

The irradiation of the dye solutions for seconds by the argon-ion laser or for microseconds by the flash resulted in a bleaching of the $\pi\pi^*$-CT band and transformation of most of the stable trans form into the cis isomer. The thermal back reaction into the trans form occurred according to a first-order rate law in all pure solvents, solvent/water mixtures, and surfactant solutions, except for some cases with dyes **I** and **IV** in bicontinuous microemulsions. Isomerization was followed by means of the PMT signal and evaluated according to equation (1) from the change in absorbance during 2 to 3 half-lifes (Fig. 1).

$$\ln \{(A_0 - A_{oo})/(A_t - A_{oo})\} = k_{iso}t \qquad (1)$$

The sequence between photochemical trans → cis and thermal cis → trans isomerization was completely reversible for several cycles which were carried out with one sample.

For repeated experiments with the same solution the standard deviation of k_{iso} was found to be less than ± 5%, and for experiments with independently prepared solutions, ± 15%.

In acetone/water mixtures (1:1, v:v) an increase of the isomerization rate constants was observed for pH < 5.2 when small amounts of HCl were added stepwise. As water/ surfactant solutions were studied at pH > 5.6, we assume that the rate constants refer to unprotonated cis isomers of the azo dyes.

It was confirmed by NMR experiments that $-NH$, $-NH_2$, and $-OH$ protons of the azo dyes and surfactants, respectively, were immediately replaced by deuterium in D_2O as a solvent.

RESULTS AND DISCUSSION

Isomerization Rate Constants in Homogeneous Solvents and Acetone/Water Mixtures

Understanding the influence of the microenvironment in water surfactant interface layers on k_{iso} requires an understanding of the influence of the microenvironment in solvents and solvent mixtures. Therefore, we began with experiments in different aprotic solvents, highly viscous polyglycols PEO(600), PPO(425), PPO(2000), and mixtures of acetone with H_2O. In Table I λ_{max}-values of the trans form and the corresponding k_{iso}-values in pure solvents are given together with available data from the literature. There is satisfactory agreement between our data and literature values where available.

The electronic effects of the substituents at the amino group on λ_{max} can be separated from other fac-

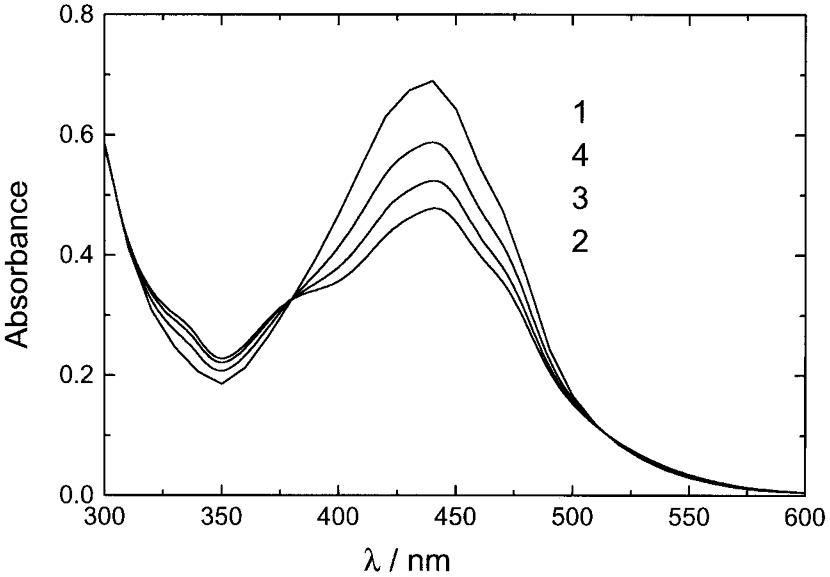

Figure 1a UV/VIS absorption spectra before and after irradiation (90 s with the 514.5 nm line) of dye **IV** in cyclohexane in an 1 cm cuvette. 1 = before irradiation and at infinite time after irradiation, 2 = 1 min, 3 = 4 min, 4 = 9 min after irradiation.

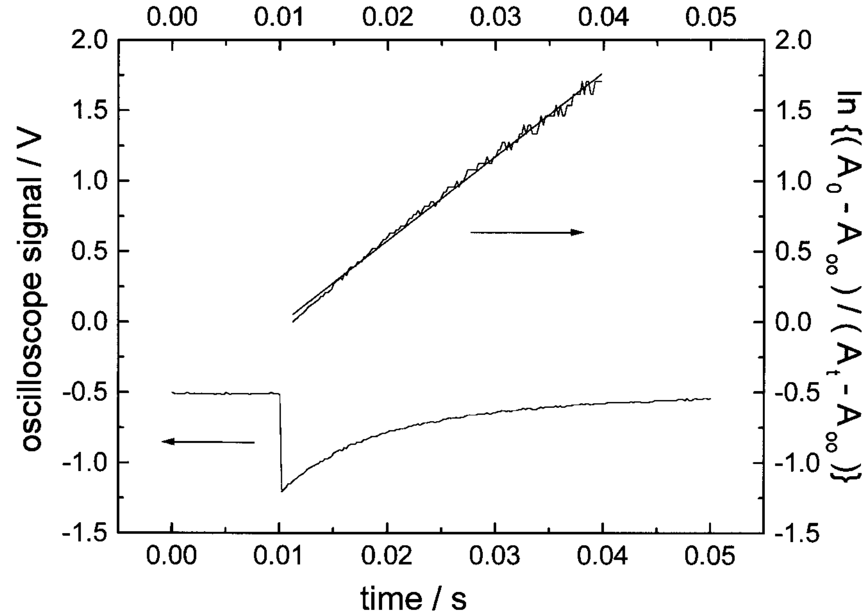

Figure 1b Oscilloscope trace before and after the microsecond flash (observation wavelength 493 nm) on dye **IV** in 4×10^{-4} mol dm^{-3} $C_{12}EO_8$; experimental data, and fit of the first-order rate law, respectively.

tors by consideration of the data determined in the unpolar aprotic solvents heptane and cyclohexane. The order of λ_{max}-values for the four dyes in both solvents is **I** < **III** < **IV** < **II**. This order reflects the increasing ability of the substituents at the amino group to stabilize the electronically excited $\pi\pi^*$ charge transfer state. This increasing electron donor ability of the substitutents at the amino nitrogen should also increasingly stabilize the bipolar transition state of the thermal cis-trans isomerization [15]. The isomerization rate constants k_{iso} increase in the order **IV** < **III** < **II** < **I**, and there is a remarkable inversion in the order of k_{iso} between **I** and **IV** compared with the order of λ_{max}. The k_{iso} order reflects the different steric requirements for rotation of the aminobenzene and the anilinobenzene group, respectively. Whereas, for the ami-

Table I UV/VIS Absorption Maxima λ_{max} and Cis-trans Isomerization Rate Constants k_{iso} at 298 K of Azo Dyes in Aprotic Solvents and Neat Polyglycol Oligomers of Viscosity η

		I		II		III		IV	
Solvent	η/mPa s	λ_{max}/nm	k_{iso}/s^{-1}	λ_{max}/nm	k_{iso}/s^{-1}	λ_{max}/nm	k_{iso}/s^{-1}	λ_{max}/nm	k_{iso}/s^{-1}
Heptane	0.386	400	8.5×10^{-3}	453	4.9×10^{-3}	430	2.5×10^{-3}	438	1.4×10^{-3}
				451	7.0×10^{-3a}				
Cyclohexane	0.896	408	8.5×10^{-3}	457	4.7×10^{-3}	430	2.4×10^{-3}	440	0.9×10^{-3}
					5.0×10^{-3a}			435	0.6×10^{-3b}
									1.6×10^{-3c}
Acetone	0.310	438	1.35	490	17	465	0.58	461	0.19
				493	18[a]			461	0.12[b]
					19[d]				0.14[c]
Acetonitrile	0.345	429	1.56	490	52	462	1.55	455	2.7×10^{-2}
				491	58[a]			456	2.0×10^{-2b}
Propionitrile	0.413	430	1.00	490	29	461	1.00	458	0.33
Butyronitrile	0.565	432	1.14	491	21	465	2.44	461	0.20
DMF	0.924	457	78	502	1.3×10^{2}	479	8.1	484	4.9
PEO 600	141	455	46	501	42	480	2.21	486	1.23
PPO 425	76	446	5.6	490	3.60	462	0.29	480	0.17
PPO 2000	335	443	1.71	483	0.59	456	0.12	476	0.12

[a] ref. [18], [b] ref. [22], [c] ref. [23], [d] ref. [24]

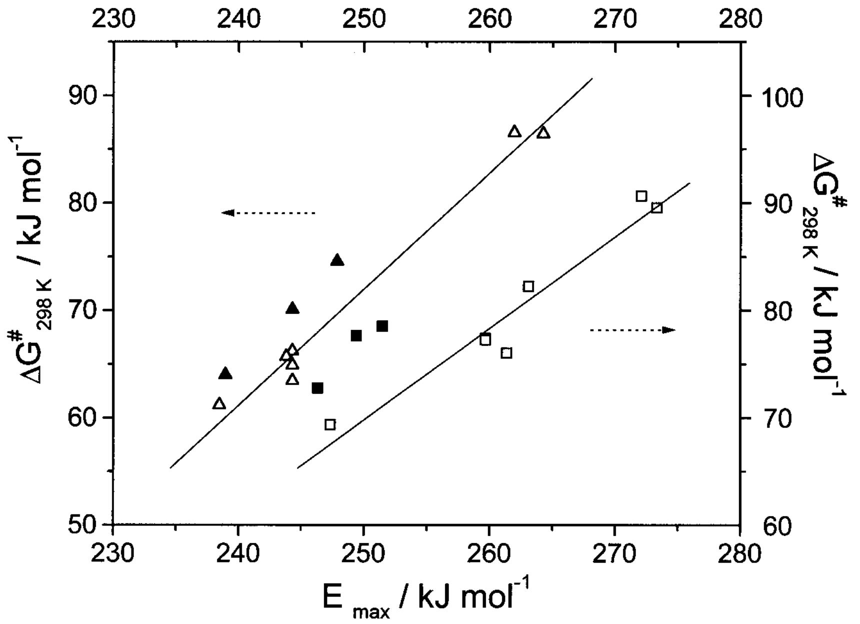

Figure 2 Plot of free activation energy of cis-trans isomerization $\Delta G^{\#}_{298\text{ K}}$ vs. E_{max} (from λ_{max}) in aprotic solvents (open symbols), PEO, and PPO's (solid symbols) for **II** (triangles) and **IV** (squares), regression lines according to eq. (2) including only aprotic solvents.

nobenzene group (in **I**), a rotor volume of about 56 ml mol^{-1} can be estimated, for the corresponding rotors (in **III, IV,** and **II**) rotor volumes of about 100 ml mol^{-1} result [25]. The order of the k_{iso}-values of **I** and **IV** is a strong indication that viscosity influences the cis-trans isomerization of azo compounds, as recently confirmed for the isomerization at carbon-carbon double bonds in bis-oxonols [26].

Before discussing the viscosity effect, the influence of the solvent polarity on the isomerization rates of particular azo dyes will be described. Several authors [14–18] have shown that polarity around donor-acceptor-substituted trans azo dyes correlates with their E_{max}-values calculated from the maximum absorbance wavelength λ_{max} ($E_{max} = h \cdot c/\lambda_{max}$, where h is the Planck constant and c is the speed of light). Therefore E_{max} is a dye specific polarity parameter. We calculated the free activation energy of isomerization $\Delta G^{\#}_{298\text{ K}} = 298\, R\{\ln(k_B 298/h \cdot k_{iso})\}$, where k_B is the Boltzmann constant and R the gas constant, as energy parameter reflecting k_{iso} at 298 K. Linear plots of $\Delta G^{\#}_{298\text{ K}}$, vs. E_{max}, according to equation (2)

$$\Delta G^{\#}_{298\text{ K}} = a + b\, E_{max} \tag{2}$$

of azo dyes, without protic hydrogen atoms in aprotic solvents, allowed separation from H-bonding effects. Azo dyes **II** and **III** fulfill this requirement. The regression parameters a and b were calculated also for **I** and **IV,** neglecting possible hydrogen bonding between the hydrogen atoms at the amino groups of **I** and **IV** and hydrogen bond acceptor groups in the aprotic solvents. In Figure 2 the data and regression lines of **II** and **IV** are shown as examples. Slopes b between 0.6 and 1.1 were determined (Table II). A slope b of about one suggests that there is a similar degree of charge transfer in the transition state for the isomerization reaction and in the Franck-Condon excited state after light absorption, as found earlier for dye **II** [15].

Table II Parameters of Equations (2) and (3) Reflecting the Polarity and Viscosity Effects on Free Activation Energy $\Delta G\#_{298}$, and ln k_{iso}, Respectively, of Cis-trans Isomerization of the Azo Dyes

Azo Dye	a	b	C	α	β[a]
I	−101 ± 16	0.63 ± 0.06	−5.60 ± 0.51	0.15 ± 0.10	−0.26 ± 0.02
II	−193 ± 17	0.85 ± 0.10	−5.76 ± 0.36	0.32 ± 0.06	−0.43 ± 0.02
III	−129 ± 12	0.78 ± 0.05	−6.06 ± 0.35	0.24 ± 0.07	−0.30 ± 0.02
IV	−142 ± 26	0.85 ± 0.10	−7.04 ± 0.49	0.52 ± 0.12	−0.35 ± 0.03

[a] $-\beta \times RT$ corresponds to parameter b.

With increasing donor ability of the amino group, that is, increasing λ_{max} of the dyes in the unpolar solvents heptane and cyclohexane, an increasing slope b was obtained. It corresponds to increasing sensitivity of the isomerization rates of the various dyes to solvent polarity. From these aprotic solvents with bulk viscosities $0.3 < \eta < 1$ mPa · s the dependence of k_{iso} on viscosity cannot be derived.

To obtain k_{iso}-values from solvents with high bulk viscosity we studied the isomerization in pure polyglycol oligomers PEO(425), PPO(600), and PPO(2000). The isomerization rates are lower and the $\Delta G^{\#}_{298\,K}$ higher than expected from the $\Delta G^{\#}_{298\,K}/E_{max}$-correlation with the aprotic solvents of low viscosity (Fig. 2). The decrease in rate at higher viscosity is obvious in these solvents, although the rate-increasing hydrogen-bonding effect of the hydroxylic end groups in PEO/PPOs cannot be considered separately. Therefore, only a lower limit of the influence of viscosity can be quantified by α, equation (3), which is similar to an equation used by Benniston and Harriman [26]. It correlates ln k_{iso} with bulk viscosity η and E_{max} as a measure of polarity. The E_{max}-value for each dye is highest in heptane and it was taken as a reference for zero polarity.

$$\ln k_{iso} = C - \alpha \ln \eta + \beta(E_{max} - E_{max0}) \qquad (3)$$

The calculated intercept C has the meaning of C = (ln B $-$ E_A/RT), whereas B is the viscosity-independent preexponential factor, and E_A is the polarity-independent Arrhenius activation energy. The α-values are empirical parameters approximately dependent on viscosity. They increase in the order **I, III** and **II, IV** (Table II), and show the difference in the rotor volumes between **I** and the other dyes. Despite similar rotor volumes, the α-values show also a difference between dyes **III**, **II**, and **IV**, respectively, probably due to the different molecular shapes of the amino groups.

All azo dyes of this study may accept hydrogen bonding at the nitro group which stabilizes both the bipolar transition state of cis-trans isomerization and the Frank-Condon state, and increases both k_{iso} and λ_{max} (and decreases E_{max}). Hydrogen bonding is likewise possible at the lone electron pair of the amino group [27], which decreases both k_{iso} and λ_{max}. Hydrogen bonding between hydrogen atoms at the amino group in **I** and **IV** with hydrogen bond acceptor groups of solvents, however, increases the donor capability of the amino group. The balance of these effects results in an increase of the isomerization rate [15] in solutions containing water. We studied UV/Vis absorption and cis-trans isomerization in acetone/water mixtures in order to derive qualitatively the hydrogen bonding effect of water on λ_{max} and k_{iso}. Differences between the azo dyes in hydrogen bonding result from differences at their amino groups.

Acetone with added water (4:1 v:v) gave an increase in λ_{max} and k_{iso} compared to pure acetone due to increasing solvent polarity (Table III). However, increasing occupation of the amino nitrogen lone electron pair by hydrogen bonding with water leads to a decrease of λ_{max} and k_{iso}. As an overall effect, a maximum in λ_{max} (at acetone water 4:1 v:v) and k_{iso} (at acetone water 1:4 v:v) was observed for dye **I.** Therefore, we conclude that an increase of polarity and hydrogen bonding may balance in λ_{max} and k_{iso}. λ_{max} reflects the electronic effects of the environment of the dye on a time average. Given the drop of λ_{max} of 19 nm on changing from acetone/water 1:4 to pure water, a large decrease of k_{iso} would be expected. However, only a small decrease of k_{iso} was observed indicating an additional rate increasing factor. This might be a favorable cooperative dynamics of hydrogen bond forming (nitro group) and breaking (amino nitrogen lone pair) with water molecules.

Only **I** is sufficiently soluble in pure water to cover the entire range of mixtures with water. The other dyes could only be studied in acetone/water mixtures $\geq$1: 4. They are less capable of hydrogen bonding at the amino nitrogen for steric reasons but seem to behave similarly, as shown for **II** in Table III. With acetone/

Table III UV/VIS Absorption Maxima λ_{max} and Cis-trans Isomerization Rate Constants k_{iso} at 298 K in Acetone/Water Mixtures (v : v)

	I		**II**	
Solvent	λ_{max}/nm	k_{iso}/s^{-1}	λ_{max}/nm	k_{iso}/s^{-1}
Acetone	438	1.4	490	17
Acetone/water				
4 : 1	448	73	502	0.88×10^3
1 : 1	441	0.64×10^3	507	2.4×10^3
1 : 4	441	2.1×10^3	508	1.1×10^3
1 : 9	435	1.7×10^3		
Water	422	1.6×10^3		

water of 1:1 a maximum of k_{iso} and a plateau-value of λ_{max} was observed.

These results from homogeneous solvents and acetone/water mixtures show that trends of the influence of polarity, viscosity, and of water in the microenvironment of the isomerizing azo dye molecules in fluid media can be interpreted.

Changes of the Microenvironment for Azo Dyes at Different Surfactant Concentrations

Anionic (SDS). By increasing [SDS] from 0.01 mol dm^{-3} (cmc = 0.008 mol dm^{-3} [28]) to 0.5 mol dm^{-3} in H_2O, and in D_2O, respectively, a considerable decrease of the rate constant of **IV** was observed (Fig. 3). Unfortunately, k_{iso} could not be determined in pure water. Therefore, it cannot be excluded that the largest values of k_{iso} at the lowest SDS concentrations contain some contribution of high rates from isomerization in water due to incomplete binding of the dye to micelles [29].

$\lambda_{max} = 492 \pm 1$ nm was constant in the entire concentration range. The constant λ_{max}-value indicates constant electronic effects around the azo dye due to constant or compensating "static" effects by micropolarity and H-bonding. Therefore, the large concentration effect on the isomerization rate might, in part, be due to viscosity changes around the reacting probe molecule. An increase of the aggregation number of SDS micelles between 63 and 89 occurs at concentrations between 0.02 and 0.2 mol dm^{-3} [28,30]. This can be expected to lead to a denser packing of the surfactant molecules and increasing microviscosity in the micelles, and therefore to a decrease of the isomerization rate of **IV**. The decrease by factor 2 in k_{iso} between 0.04 and 0.05 mol dm^{-3} in H_2O is in accord with a result from the literature, where in the same concentration range cis-trans isomerization of 4,4'-nitro-dimethylaminoazobenzene showed the strongest decrease of k_{iso} on stepwise increasing SDS concentrations [31].

For the solvent kinetic isotope effect, $k_{iso}(H_2O)/k_{iso}(D_2O) = 2.1 \pm 0.1$ was determined at [SDS] < 0.040 mol dm^{-3} and 1.0 ± 0.2 at [SDS] > 0.040 mol dm^{-3}. The large kinetic solvent isotope effect at [SDS] ≤ 0.04 mol dm^{-3} indicates a better access of water to the microenvironment of the probe molecules at lower SDS concentrations. A possible dynamic H-bonding effect decreases with decreasing access of water to the dye molecules. This might also contribute to the decrease of k_{iso} at [SDS] ≥ 0.04 mol dm^{-3} (Fig. 3).

Within the same concentration range of SDS, azo dye **I** behaves similarly to **IV**. At constant λ_{max} = 445 ± 1 nm, k_{iso} decreases less for **I** than **IV,** from 1344 (0.01 mol dm^{-3}) to 232 s^{-1} (0.2 mol dm^{-3}),

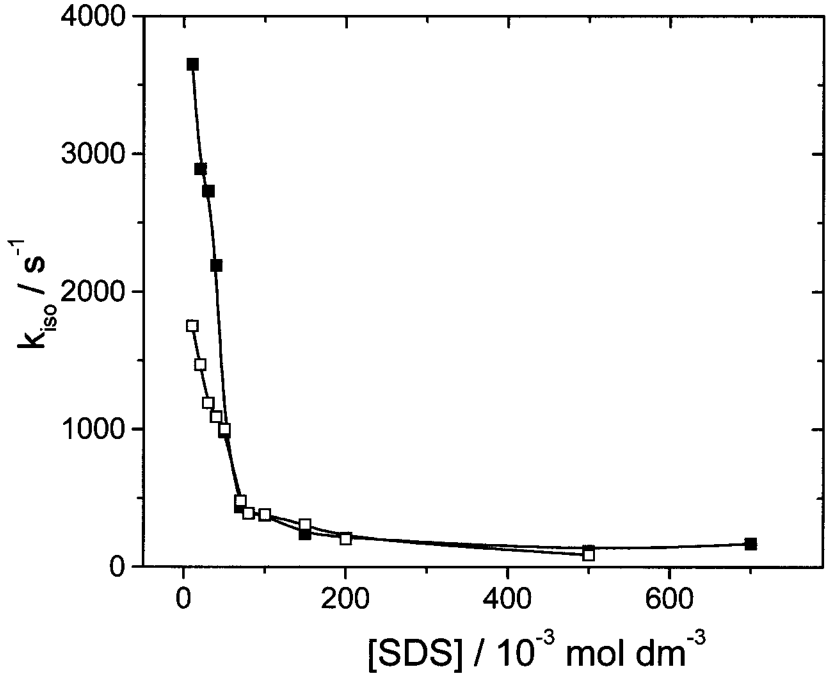

Figure 3 Plots of cis-trans isomerization rate constants k_{iso} of **IV** at 298 K vs. SDS concentration in H_2O (full squares), and D_2O (open squares), respectively. Lines are guides for the eye.

whereas $k_{iso}(H_2O)/k_{iso}(D_2O)$ changes from 1.6 ± 0.2 in the lower concentration range to 1.3 ± 0.2 in the higher concentration range. Unlike dye **IV,** dye **I** is water soluble, and incomplete binding to the micelles occurs in the lower concentration range. Therefore, only data from the higher concentration range can be compared with the results of dye **IV**. The λ_{max}-value corresponds to an acetone/water mixture of about 2:1. Moreover, the isotope effect and k_{iso}-values indicate the presence of water for **I** in all solutions and a solubilization site of **I** at the water side of the water surfactant interface.

Nonionic/triton X-100. Due to the better solubility of the azo dyes by triton X-100 compared to SDS micelles, solubilization and reduction of k_{iso} begins below the cmc for **IV** (Fig. 4). This decrease can only be explained by assuming the existence of premicellar aggregates. Recent papers give indications of premicellar aggregates for nonionic surfactants [1,32]. It is an open question if such premicellar aggregates exist without the probe molecules or if these molecules induce aggregations [33–36].

Although the λ_{max}-values of 493 ± 1 nm were constant between 0.5 and 20 times the cmc, indicating constant (or balancing) micropolarity and extent of hydrogen bonding, there was a decrease of one order of magnitude in k_{iso}. Again, this might be due to an increase of microviscosity with increasing surfactant concentration and increasing aggregation numbers, as in the case of SDS, although no such data are available for the low triton X-100 concentrations of this study. Again, the most interesting fact is a clear break in the values for the isotope effect, from about (5 ± 1) at [triton] $<$ 2 cmc to about (2.6 ± 0.7) at [triton] $\geq$ 2 cmc. This might reflect a more rigid solvent structure/higher viscosity of micellar aggregates in D_2O and a persisting solubilization site of **IV** within the water containing polyethyleneoxide headgroup shell.

D_2O is the usual solvent in studies of aggregation behavior of amphiphiles by means of NMR [37] and neutron scattering. However, experimental effects caused by the exchange of H_2O by D_2O in surfactant/water and lipid/water mixtures have been studied only occasionally. Some general conclusions from such investigations are that hydrophobic and electrostatic interactions between hosts (e.g., cyclodextrins) and guests are stronger in D_2O [38], and that the increase of the aggregation number and decrease of cmc in D_2O [39] compared to H_2O, phase diagrams of mixtures from H_2O and D_2O, respectively, are not very different [40]. Our results show that small differences in structure and equilibria properties may be amplified in kinetic parameters. Differences in H_2O and D_2O solutions, respectively, are also evident in the slightly better solubility of the azo dyes in D_2O solutions compared to H_2O solutions at the same lowest triton X-100 concentrations used.

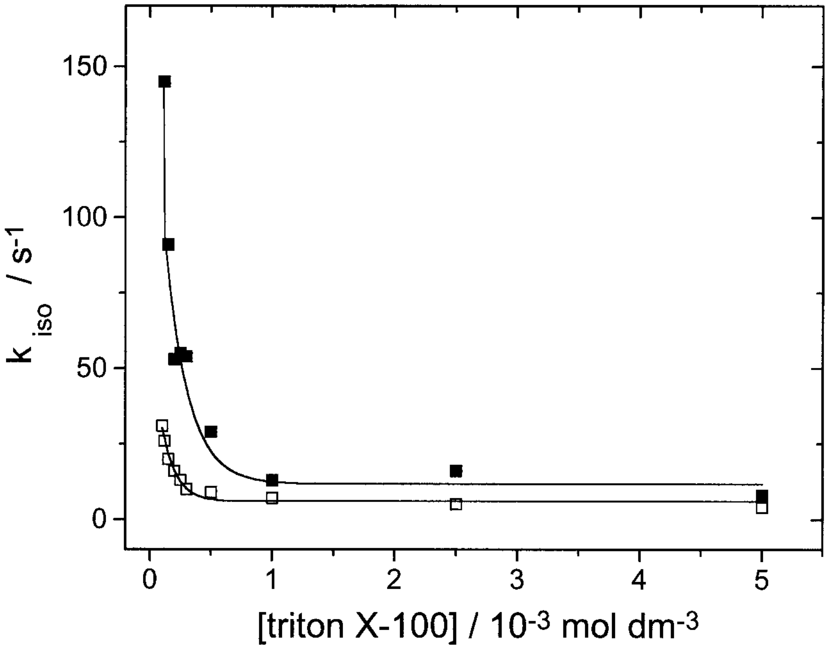

Figure 4 Plots of cis-trans isomerization rate constants k_{iso} of **IV** at 298 K vs. triton X-100 concentration in H_2O (full squares), and D_2O (open squares), respectively. Lines are guides for the eye.

Table IV UV/VIS Absorption Maxima λ_{max} and Cis-trans Isomerization Rate Constants k_{iso} at 298 K of I in Dependence on the Triton X-100 Concentration

[Triton X-100]/ 10^{-4} mol dm^{-3}	H_2O		D_2O		
	λ_{max}/nm	$k_{iso}/10^3$ s^{-1}	λ_{max}/nm	$k_{iso}/10^3$ s^{-1}	k_{H2O}/k_{D2O}
1.0	426	3.0	426	1.2	2.5
1.2	427	2.9	428	1.2	2.4
2.0	436	3.0	433	1.5	2.0
5.0	456	2.4	453	1.1	2.2
10	460	2.1	453	1.2	1.7
25	460	1.7			
50	462	1.3			

Table IV gives the data for **I** in triton X-100, which show quite different trends compared with those of **IV**. λ_{max} is 426 nm below the cmc, which indicates an environment similar to acetone/water 1:9 (see Table II), but k_{iso} is twice as high as in pure water, obviously due to interactions with premicellar triton X-100 aggregates. λ_{max} increases with increasing triton X-100 concentration, in part probably because of more complete binding to micelles. On the other hand, the isomerization rate constant decreases only by a factor of two. The increase in λ_{max} might be due to a change in the orientation of the amino group in **I** from the water side with a high chance of hydrogen bonding (acceptor) onto the micelle interior at higher surfactant concentrations. The small change of k_{iso} with [triton X-100] is in accord with the lower sensitivity of k_{iso} of **I** to changes in microviscosity, so that the microviscosity does not change as much at the solubilization site of **I** in triton X-100 solutions compared to the microenvironment of **IV**. The change of λ_{max} and k_{iso} of **I** between 2 and 5 × 10^{-4} mol dm^{-3} of triton X-100, however, reflects clearly the structure changes caused by micelle formation.

$C_{12}EO_8$. The dependence of the isomerization rate constant of **IV** on the concentration of $C_{12}EO_8$ above the cmc is shown in Figure 5. There is a similar decreasing kinetic solvent isotope effect with increasing

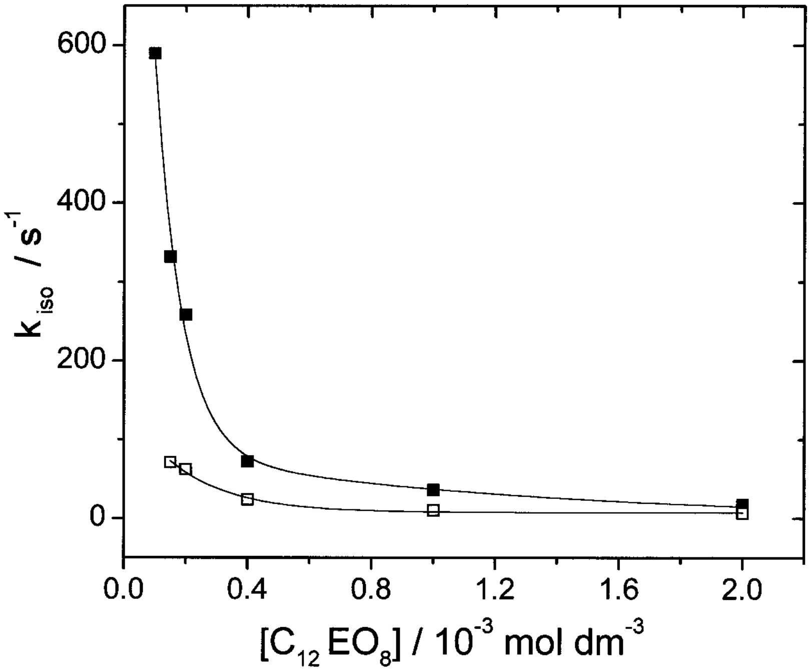

Figure 5 Plots of cis-trans isomerization rate constants k_{iso} of **IV** at 298 K in dependence of $C_{12}EO_8$ concentration in H_2O (full squares), and D_2O (open squares), respectively. Lines are guides for the eye.

surfactant concentration as in triton X-100 solutions. The constant λ_{max}-value of 493 nm of **IV** in both $C_{12}EO_8$ and triton X-100, and the absence of a vanishing kinetic solvent isotope effect at high surfactant concentrations indicate a similar solubilization site in the water-surfactant interface layers on increasing concentrations of both surfactants. The decrease in k_{iso} in the concentration range between the cmc (for triton X-100 at 2.5×10^{-4} mol dm$-^{3}$ [41], for $C_{12}EO_8$ at 1.0×10^{-4} mol dm^{-3} [42]) and 20 cmc for both surfactants is about sixfold for triton X-100, and thirtyfold for $C_{12}EO_8$ (Figs. 4 and 5). The phenyl group in triton X-100 may anchor **IV** in the micelles fixing the anilino group of the dye in a microenvironment of higher viscosity at lower surfactant concentrations compared to $C_{12}EO_8$.

Cis-trans Isomerization in Bicontinuous Microemulsions

Bicontinuous microemulsions have a sponge-like microstructure between swollen micelles and reverse micelles. They have been used as reaction media only recently [2,43,44]. To the best of our knowledge, cis-trans isomerization of azo dyes has not yet been studied in such surfactant media. Different from micellar solutions, beside the extended water/surfactant interface layer a large volume of unpolar oil domains may dissolve the dye molecules and distributions between different solubilization sites must be considered. We prepared transparent bicontinuous microemulsions of different compositions within the one-phase region from igepal CA-520, heptane and water, based on a published phase diagram [45]. Igepal CA-520 structure is similar to that of triton X-100, but has an unbranched hydrocarbon tail. The experimental results are summarized in Table V.

In all four microemulsions studied, azo dye **I** shows $\lambda_{max} = 437$ nm, which indicates a less polar average solubilization site than in micellar triton X-100 solutions (≈ 460 nm). Considerable deviations from the first-order rate law according to eq. (1) were obtained. From absorbance/time curves $(A_{oo} - A_t)/(A_{oo} - A_0)$ was calculated, which corresponds to the concentration ratio of cis isomers at times *t* and zero, respectively. Its dependence on time is shown in Figure 6. The curves could not be fitted to a biexponential rate law, but reasonable fits according to eq. (1) were obtained with estimated A_{oo}-values for the first part of the curves. These k_{iso}-values are given in Table V. They are an order of magnitude smaller than those in triton X-100 solutions (See Table IV).

The $(A_{oo} - A_t)/(A_{oo} - A_0) = f(t)$ curves change with the wavelength range of exciting light λ_{exc} for the trans-cis isomerization and observation wavelength λ_{obs} for the thermal cis-trans isomerization of **I** (Fig. 6). With a blue flash filter ($350 < \lambda_{exc} < 480$ nm) more cis **I** can be prepared in heptane domains than with a green flash filter ($\lambda_{exc} > 430$ nm). With $\lambda_{obs} = 400 \ldots 420$ nm mainly low polar domains were monitored. About 50% "slow" isomerization was observed using the blue flash filter, but only about 15% ($\lambda_{obs} = 420$ nm) was observed with the green flash filter. Nethertheless, this "slow" isomerization is com-

Table V UV/VIS Absorption Maxima λ_{max} and Cis-trans Isomerization Rate Constants k_{iso} at 298 K of Azo Dyes in Bicontinuous Microemulsions A, B, C, and D from Igepal CA-520/Heptane/Water[a]

Azo Dye/ Microemulsion		H_2O		D_2O		
		λ_{max}/nm	k_{iso}/s^{-1}	λ_{max}/nm	k_{iso}/s^{-1}	k_{H2O}/k_{D2O}
I	A	437	139	434	109	1.3
	B	437	141			
	C	437	148			
	D	437	206			
II	A	463	172	464	105	1.6
	B	462	165			
	C	460	171			
	D	480	505			
IV	A	485	2.13	482	1.55	1.4
	B	484	2.01			
	C	484	2.45			
	D	484	5.5			

[a] Microemulsion compositions: igepal CA-520/heptane/water in weight percent: A (20 : 40 : 40), B (20 : 35 : 45), C (20 : 50 : 30), D (25 : 30 : 45) with H_2O, and A (19.2 : 38.3 : 42.5) with D_2O, to have equal molar ratios in A with both H_2O and D_2O. Bulk viscosities at 298 K in mPas were A, 34; B, 34; C, 18; and D, 48. Small amounts of 0.1 mol dm^{-3} NaOH were added to adjust pH > 6.0.

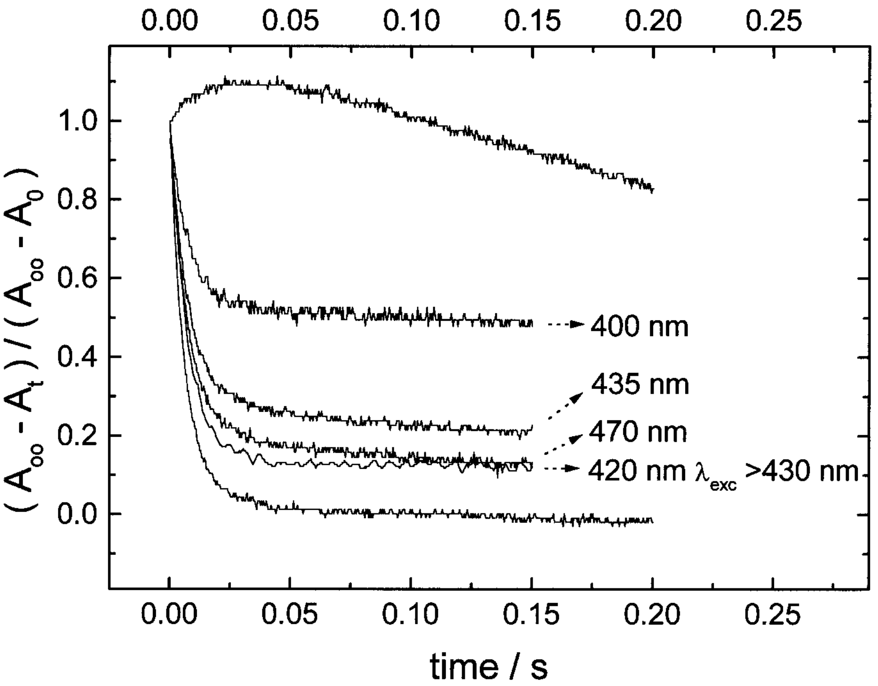

Figure 6 Plots of $(A_{oo} - A_t)/(A_{oo} - A_0)$ vs. time for three dyes in microemulsion A. Dyes **II** and **IV** ($\lambda_{exc} > 430$ nm) show curves independent on λ_{obs} and λ_{exc}. Data determined at $\lambda_{obs} = 400$, 435, and 470 nm for **I** were obtained with a blue flash filter ($350 < \lambda_{exc} < 480$ nm).

plete within a few seconds and therefore much faster than would be expected for cis-trans isomerization in pure heptane (see Table I). Therefore, we assume that the second branch of the $(A_{oo} - A_t)/ (A_{oo} -- A_0) = f(t)$ curve originates from the isomerization rate determining redistibution of cis isomers into the polar surfactant water interface. By increasing λ_{obs} to 435 and 475 nm (blue flash filter), more polar domains were monitored and the relative contribution of the slow component decreased.

II is the most hydrophobic dye studied and mainly solubilized in a low polar environment as $\lambda_{max} \approx 460$ nm in microemulsions A, B, and C shows, compared to $\lambda_{max} = 505$ nm in micellar triton X-100 solution ($k_{iso} \approx 4 \cdot 10^3\ s^{-1}$). Only microemulsion D, with the highest content of surfactant $\lambda_{max} = 480$ nm, indicates a more polar microenvironment. All isomerization rate constants are larger than expected from the λ_{max}-values in Table I. In contrast to **I** the kinetic curves of **II** are monoexponential up to about 95% conversion and independent of excitation and observation wavelength. A fast redistribution of the cis isomer into polar water containing domains with faster isomerization rates can be assumed. The same conclusion had been drawn from isomerization experiments with **II** in reverse micellar solutions of AOT [18]. However, the difference in redistribution behavior between **I** (slow) and **II** (fast) cannot be explained from our results.

There is an initial increase of cis **IV** at 450 nm $< \lambda_{obs} <$ 525 nm until about 30 ms after the flash, which shows that a small part of the cis isomer was redistibuted before isomerization (Fig. 6). Decreasing values $(A_{oo} - A_t)/(A_{oo} - A_0) \leq 1$ at reaction times > 0.1 s were used for calculation of first-order rate constants (Table V). A dependence of rate constants on different flash filters and on observation wavelength was not found. $\lambda_{max} \approx 484$ nm reflects a moderate polar microenvironment and rate constants between 2.0 and 5.5 s^{-1} in the microemulsions with H_2O are comparable to $k_{iso} = 8\ s^{-1}$ in the 5 mmol dm^{-3} solution of triton X-100. Dye **IV** has the lowest isomerization rate constants of all dyes studied in bicontinuous microemulsions because it has the strongest sensitivity to microviscosity and because of possible fixation by the anilino group at the phenyl group of igepal CA-520. However, the rate constants for **IV** in microheterogeneous bicontinuous microemulsions do not correlate with their bulk viscosities (Table V). In the case of **IV,** redistribution occurs before most of the cis isomer can isomerize due to the slow isomerization rate of **IV**.

K_{iso} of all three dyes is largest in microemulsion D with the highest content of surfactant and correspondingly the largest volume of the water/surfactant interface layer. The kinetic solvent isotope effect $k_{iso,\ H2O}/k_{iso,\ D2O} \approx 1.4$ (fast component) proves that water has access to all three isomerizing dyes in microemulsion

A and that isomerization occurs in the water/surfactant interface layer.

SUMMARY AND CONCLUSIONS

The influence of polarity and bulk viscosity on the rate constants of the thermal cis-trans isomerization of 4,4'-nitroaminoazobenzenes were estimated quantitatively from λ_{max} ($\pi\pi^*$ CT-transition of the trans forms) in homogeneous solvents and in solvents of high bulk viscosity.

The influence of increasing concentration of water in the microenvironment of the azo dyes on λ_{max} and k_{iso}, respectively, is threefold and can be described qualitatively: increase of polarity (positive for λ_{max} and k_{iso}), decrease of the electron donating ability of the amino group due to H-bonding at the nitrogen electron lone pair (negative for λ_{max} and k_{iso}), and increasing influence of another factor, possibly dynamics of hydrogen bond forming and breaking steps on k_{iso} (positive, by favorable charge fluctuations).

According to the λ_{max}-values, the trans azo dyes have a constant, or with respect to polarity and hydrogen bonding, balancing average microenvironment in the water/surfactant interface layer in a wide range of micelle concentrations. The isomerization rates of their cis isomers decrease up to an order of magnitude with increasing surfactant concentration, in part due to increasing microviscosity.

The large kinetic solvent isotope effects at equal surfactant concentrations in H_2O, and D_2O solutions, respectively, are caused by differences in structures dominated by hydrogen bonding. They give a clear indication about the presence of water in the microenvironment of the reacting azo dyes.

In bicontinuous microemulsions of igepal CA-520/water/heptane the azo dyes studied may be solubilized at different sites mainly in the extended pseudophases oil and water/surfactant interface. Deviations from first-order behavior indicate redistribution between different solubilization sites.

The k_{iso} increasing effects of hydrogen bonding and structural fluctuations of the water/surfactant interface layer could not be separated.

K. G. gratefully acknowledges a grant and further support by the Graduiertenkolleg "Physikalische Chemie der Grenzflächen" at the University of Leipzig, sponsored by Deutsche Forschungsgemeinschaft and Sächsisches Staatsministerium für Wissenschaft und Kunst. We thank R. Wang for some measurements and the Fonds der Chemischen Industrie for financial support.

BIBLIOGRAPHY

1. Cho, C. H.; Chung, M.; Lee, J.; Nguyen, T.; Singhh, S.; Vedamurthu, M.; Yao, S.; Zhu, J.- B.; Robinson, G. W. J Phys Chem 1995, 99, 7806.
2. Schwuger, M.-J.; Stickdorn, K.; Schomäker, R. Chem Rev 1995, 95, 849.
3. Tsukamoto, I.; Ogli, K. J Colloid Interface Sci 1994, 168, 323.
4. Saroja, G.; Samanta, A. Chem Phys Lett 1995, 246, 506.
5. Miyagishi, S.; Asakawa, T.; Nishida, M. J Colloid Interface Sci 1995, 115, 199.
6. Miyagishi, S.; Kurimoto, H.; Ishihara, Y.; Asakawa, T. Bull Chem Soc Jpn 1994, 67, 2398.
7. Miyagishi, S.; Kurimoto, H.; Asakawa, T. Bull Chem Soc Jpn 1995, 68, 135.
8. Yao, J.; Romsted, L. S. J Am Chem Soc 1993, 115, 8351.
9. Romsted, L. S.; Yao, J. Langmuir 1996, 12, 2425.
10. Garcia-Ris, L.; Leis, J.-R.; Iglesias, E. J Phys Chem 1995, 99, 12318.
11. Szadjdzinska-Pietek, E.; Gebicki, J. L. J Phys Chem 1995, 99, 13500.
12. Mancini, G.; Schiavo, C.; Cerichelli, G. Langmuir 1996, 12, 3567.
13. Kluge, T. AM1 calculations, unpublished.
14. Schanze, K. S.; Mattox, T. F.; Whitten, D. G. J Am Chem Soc 1982, 104, 1733.
15. Schanze, K. S.; Mattox, T. F.; Whitten, D. G. J Org Chem 1983, 48, 2808.
16. Schanze, K. S.; Whitten, D. G. J Am Chem Soc 1983, 105, 6734.
17. Shin, D.-M.; Whitten, D. G. J Am Chem Soc 1988, 110, 5206.
18. Shin, D.-M.; Schanze, K. S.; Whitten, D. G. J Am Chem Soc 1989, 111, 8494.
19. Abdel-Halim, S. T.; Abdel-Kader, M. H.; Steiner, E. U. J Phys Chem 1988, 92, 4324, and private comm. by Prof. Steiner.
20. Beilsteins Handbuch der Organischien Chemie, Vol 16, 314, Springer-Verlag Berlin, 1933.
21. Landoldt-Börnstein, Vol II/5a, 6th ed., 1969, Springer-Verlag, Berlin.
22. Kobayashi, S.; Yokohama, H.; Kamei, H. Chem Phys Lett 1987, 138, 333.
23. Hair, S. R.; Taylor, G. A.; Schultz, L. W. J Chem Educ 1990, 67, 709.
24. Marcandalli, B.; Pelliciari-Di Liddo, L.; Di Fede, C.; Bellobono, J. R. J Chem Soc, Perkin Trans 1994, 2, 589.
25. Bondi, A. J Phys Chem 1964, 67, 441.
26. Benniston, A. C.; Harriman, A. J Chem Soc, Faraday Trans 1994, 90, 2627.
27. Vinogradov, S. N.; Linnell, R. H. Hydrogen Bonding; Van Norstrand Reinhold Comp.: New York 1971.
28. Bales, B. L.; Almgren, M. J Phys Chem 1995, 99, 15153.
29. A reviewer called our attention to the possibly incomplete binding at our lowest surfactant concentrations with reference to results of ref. [31].
30. Quina, F. H.; Nasser, P. M.; Bonilha, J. B. S.; Bales, B. L. J Phys Chem 1995, 99, 17028.

31. Miyagishi, S.; Matsumura, S.; Asahara, T.; Nishida, M. J Colloid Interface Sci 1988, 125, 237.
32. Uppu, R. M. Langmuir 1995, 11, 1038.
33. Kato, T.; Kanada, M.; Seimiya, T. Langmuir 1995, 11, 1867.
34. Kusumoto, Y.; Shizuke, M.; Ssataku, I.; Kagoshima, K. Chem Lett 1986, 529.
35. Seret, A.; Gandio, E.; Van de Vorst, A. Chem Phys Lett 1987, 135, 427.
36. Loran, C. P.; Von Wandruszka, R. Talanta 1991, 38, 497.
37. El Seoud, O. A.; Blasko, A.; Bunton, C. A. Langmuir 1994, 10, 653.
38. Wang, A. S.; Matsui, Y. Bull Chem Soc Jpn 1994, 67, 2917.
39. Chang, N. J.; Kaler, E. W. J Phys Chem 1985, 89, 2996.
40. Baglioni, P.; Dei, L.; Gambi, C. M. C. J Phys Chem 1995, 99, 5035.
41. Mean value of the data given in K. Kalyanasundaram, Photochemistry in Microheterogeneous Systems; Academic Press, 1987 and Catalog Sigma Chemie GmbH, 1996.
42. Heerklotz, H.; Binder, H.; Lantzsch, G.; Klose, G. Biochem Biophys Acta 1994, 1196, 114.
43. Schomäker, R.; Stickdorn, K.; Knoche, W. J Chem Soc, Faraday Trans 1991, 87, 847.
44. Jóhannson, R.; Almgren, M. Langmuir 1993, 9, 1259.
45. Grätz, K.; Helmstedt, M.; Meyer, H. W.; Quitzsch, K. Colloid Polym Sci 1998, 276, 131.